Journal of Advances in Science and Technology
Vol. 18, Issue No. 2, September–2021, ISSN 2230-9659

Design and Modeling of Electrostatically Actuated Microgripper based on Cantilever

Shubham Dubey[1]*, Dr. Girish Padhan[2]

[1] Research Scholar, Shri Krishna University, Chhatarpur M.P.

[2] Associate Professor, Shri Krishna University, Chhatarpur M.P.

Abstract - Bio-manipulation techniques and methods like optical pin, acoustic traps, magnetic tweezers, hydrodynamic fluxes and pipettes are potent for basic micro-applications will be used in the study. Challenging concepts, which involve careful design and study of devices like microfluids (Khan et al 2010) are to choose, handle and release micron-sized items in the field of robotics and to biomanipulate and assemble micro components. The microsurgery on equipment will be based on the microsurgery theory, that will uses the microgripper force to grasp the items. Microgrippers produced in recent years will be highly useful to micromanipulate biological samples. It will be operated by various processes of actuation

Keywords - Design, Modeling, Electrostatically, Microgripper, Cantilever

----------X----------

INTRODUCTION

Micro Electro Mechanical Systems (MEMS) are a cutting-edge miniaturisation technology. It is moreover recognised as the dominant and advancing technology of the twenty-first century. It is seen as an inevitable tendency in the growth of smart systems with tiny sensor impregnation as well as the creation of industrial goods. MEMS has made the most remarkable and unique advancement. Due to the emergence of several silicon-based technologies and the contributions of particular periodic table elements, MEMS advances quickly in the field of product development. Intelligent, versatile, sturdy, and affordable industrial goods are in high demand for MEMS devices.

Due to its ease of usage, minimal mechanical component requirements, and need for 0 to 6 volts of electrostatic potential level for actuation, electrostatically actuated devices form a broad spectrum of MEMS devices. Basic MEMS microstructures include microcantilever beams, microplates, and micromembranes. Microcantilevers and two end fixed beams with electrostatic actuation were employed in the design of capacitive switches and resonant sensors made using MEMS technology. The growth of MEMS-based switches is now occurring quickly, and RF switches have further advantages over solid-state switches, such as low power consumption, excellent isolation, and low insertion loss. Mechanical components that are activated by electrostatic forces are the fundamental components of MEMS switches. Electric circuits are kept running by electrostatic forces.

Due to the fact that it is compatible with microfabrication, this actuation technique is often used to drive MEMS devices (Haluzan et.al.2010). There are two types of these actuators: cantilever beams and fixed-fixed beams. Micro beams that are electrostatically activated are often employed in MEMS devices. These actuators are used in a variety of devices, including switches (Goldsmith et al. 1996), optical micro-mirrors (Hung & Senturia 1999), microwave variable capacitors (Klymyshyn et al. 2007 and Jung et al. 2001), and valves (Huff et al. 1990) for microfluidic applications.

Two parallel plates, often with two beam arrangements, make up an electrostatic actuator's capacitor. In the electrostatic actuator, one beam is fixed while the other beam or plate is free to move thanks to the microcantilever. The applied voltage between the two plates generates an electrostatic force between them, which causes the free plate or beam to deflect in the direction of the fixed plate. The electrostatic force crosses over the elastic restoring force created inside the deformed plate and impacts the fixed plate as the applied voltage is raised further. known as the pull-in effect. The pull-in voltage associated with this phenomenon is a key parameter employed in many modelling methodologies and systems.

Pull-in voltage is a key factor in electrostatic MEMS design because, in some applications, such as microphones (Pedersen et al. 1998) and pressure sensors (Ho et al. 2000 and Sallese et al. 2001), it is crucial to overcome the pull-in because, when it occurs, two plates come into contact and could

result in a short circuit and device failure. However, in other situations, such as optical systems (Chik 1997), the applied voltage is specifically adjusted or optimised such that it activates or deactivates the switch when the plate comes into contact with the substrate. Therefore, accurate modelling of electrostatic devices needed knowledge of the device's shape in order to either resolve the pull-in or make use of it for the intended purpose.

Senturia (2000) uses the parallel plate approximation approach to determine the pull-in voltage of a microcantilever beam. As a result, the author has proposed a technique in which an area of the microcantilever is subjected to electrostatic force. It has been shown that the pull-in happens when the moveable plate surpasses one third of the original airgap. This approach eliminates the impacts of fringe fields.

However, Rabaey (1996) came to the conclusion that an actuator's overall capacitance might be raised by a factor of 1.5 to 3. The device's 20 percent inaccuracy is determined using parallel-plate approximation. (1995 Osterberg).

Pamidighantam et al. (2002) produced a closed-form formula to calculate the pull-in voltage for various beams using a straightforward mass-spring-damper system. The suggested model incorporates a variety of factors, including partial electrode design, axial tension, non-linear stiffening, charge re-distribution, and fringing fields. To assess fringe field effects, a useful value of width is utilised. The outcomes of the closed-form models are examined in light of the outcomes of CoventorWare (Coventor 2010). However, the findings of their model contain up to 12.84 percent of inaccuracy. For a large variety of cantilever beam diameters, the conclusions of the model have not been independently confirmed.

Osterberg et al. (1994) developed a three-dimensional analytical model, a two-dimensional finite difference model, and a one-dimensional lumped parallel plate spring model. These models were used to describe the behaviour of circular plate microstructures, cantilever beams, and beams with two fixed ends. The CoSolve-EM simulator is used to compare the findings of the proposed model to a three-dimensional numerical computer model. However, the impact of changing the dimensions is not taken into account.

MATERIAL AND METHODS

Microgripper modeling

- **Displacement Analysis**

One of the most basic actuation-based grippers is the electrostatic gripper. The comb drive is the primary component of these actuators. Two combs, one that is mobile and the other that is stationary, make up comb drives. When voltage is supplied between two combs, a force is created that causes the moveable comb to move.

By adjusting the applied voltage in comb-drives, the electrostatic force may be regulated (Khan et al 2010). The usual design arrangement of a combdrive is shown in Figure 3.40. There are two different movement configurations, Transverse, and Lateral. For applications requiring a microgripper, lateral comb-drive is employed (Khan et al 2010).

The applied voltage and the finger shape both influence the amount of force in a microgripper. Given a constant distance between the stationary and moving fingers, rectangular fingers provide a constant force. However, once the fingers engage, the distance between them varies in those with shaped fingers. As a result, the force is likewise changed.

Additionally, the ideal finger-shaped gripper is built and studied. Additionally, FEM simulations are used to verify the microgripper and its displacement, and the simulation findings are contrasted with those obtained via analysis. Figure 3.41 from IntelliSuite depicts the simulation of the microgripper with the rectangular finger. Table 3.33 lists the gripper's component pieces, while Table 3.34 lists its dimensions. Because the smallest feature size that could be created was 5 m, the finger size had to be expanded, resulting in a 10 m gap between the fingers. The microgripper is then created, and its effectiveness is examined.

- **Load Analysis of Microgripper**

To gauge the force grippers apply while grabbing an item, a microgripper force model is created. The weight of the item being lifted serves as the model's input, and its output is the amount of force the gripper must apply in order to firmly hold that thing.

Using the following method, the gripper's analysis with load is conducted. Weight of the item being lifted is the model's input.

The output is the amount of force required by the finger to firmly hold that item. Here, it is assumed that the item is spherical, like a dried red blood cell. Equation (1) provides the gripper's force.

Force exerted by the gripper

$$F = \frac{mg_l}{2\mu_1 \cos\theta - 2\sin\theta} \quad \ldots\ldots(1)$$

Where, m =mass of the load in kg

g_l =Gravitational constant 9.8m/s2

μ1 = frictional coefficient between gripper and load

θ =Angle between the load and gripper.

Calculation of force/contact area (Pressure) is described below.

Load or objects aimed to grip: Dried red blood cell

Diameter of one red blood cell = 8 µm.

Mass of one red blood cell =27picogram

μ_l = 0.38

Angle between the load and jaw = 35◦

Using Equation (4.1), Force exerted = 2 x 10^{-6} N

Surface area of gripper jaw = 50 µm

Pressure = Force exerted /Surface Area = 0.0312 Pa.

Simulation is done using IntelliSuite software (IntelliSuite 2007) with this value of pressure applied on the jaws of the gripper.

- **Fem simulation of microgripper using intellisuite**

For the purpose of microfabrication, 2D masks are produced using IntelliMask. GDSII and DXF formats may be used to import masks. To create the necessary mask files, all the fundamental forms are accessible. The planned layouts may be imported from the mask file into a 3-D builder to add height information or into IntelliFab to see the virtual manufacturing process in action.

An IntelliSuite module called the 3D Builder is used to create and mesh the three-dimensional geometry of MEMS systems. The 3-D structure may be created after importing the mask plan from IntelliMask. The necessary model may be created immediately using a 3-D builder and a collection of layers. The mesh's fundamental building components are the elements. The analysis cannot be performed if the mesh is incompatible.

IntelliSuite does automated meshing. Global mesh refinement will result from this automated meshing. However, because both the mechanically important and non-mechanically important parts will be improved, this is undesirable. Local meshing is thus chosen. The two accessible local meshes are mechanical and electrostatic meshing. A 3-D brick solid element is used in the mechanical mesh. However, the triangular surface element is used in the electrostatic mesh. It is necessary to conduct a mesh convergence research by undertaking a number of analyses and mesh refinements.

The coupled electromechanical analysis known as thermoelectrical is utilised to determine the displacement for the applied voltage. It combines the boundary element and finite element techniques.

Analytical modeling of the microgripper

Electrostatic force is calculated using the force equation given in Equation (2).

$$F = \frac{\varepsilon_0 n t V^2}{g} \quad \text{.....(2)}$$

where, ε_0 = permittivity,

n =number of fingers,

t =thickness of finger,

g =gap distance between fingers,

V =applied voltage.

Equation contains the spring constant (k) (3).

$$k = \frac{Ewt^3}{4l^3} \quad \text{..... (3)}$$

where, w width of the beam and l length of the beam. Then, the displacement (x) is calculated using the Equation (4)

$$F = kx \quad \text{.....(4)}$$

Comparisons are made between the simulation-derived displacement findings and the analytically determined displacements. With a maximum percentage error of 1.2 percent, it is determined that both findings are in excellent agreement.

RESULT AND DISCUSSION

Pull-in Analysis of Microgripper

To determine the pull-in voltage of the electrostatically activated microgripper, closed form models are also used. The FEM model of the rectangular microgripper is seen in Figure 1. The CoSolve (coupled analysis of MemMech and MemElectro) feature of CoventorWare is utilised to find the microgripper's pull-in voltage, much as the cantilever beam simulation. Table 1 provides the pull-in voltage comparison for the rectangular microgripper.

Figure 1: FEM simulation of the pull-in analysis in Coventor Ware

Table 1: Pull-in voltage and % Error comparison for the microgripper

Dimension: Length of finger 15 μm, Width of finger w =1 μm, Gap between the fingers d_0 = 10 μm, w/d_0 = 0.1 μm					
Models	**$V_{PI, 1}$**	**$V_{PI, 3}$**	**$V_{PI, 4}$**	**$V_{PI, 5}$**	**Coventor**
Pull-in voltage	29.331	38.898	24.612	27.346	29.688
%Error	**1.202**	7.886	31.032	17.097	-

Displacement Analysis of Microgripper

IntelliSuite simulates the microgripper with the suggested finger shape. It is also simulated to confirm the rectangular finger microgripper's consistent displacement behaviour. Figures 2 to 6 display the simulation results demonstrating the displacements of microgrippers for various forms.

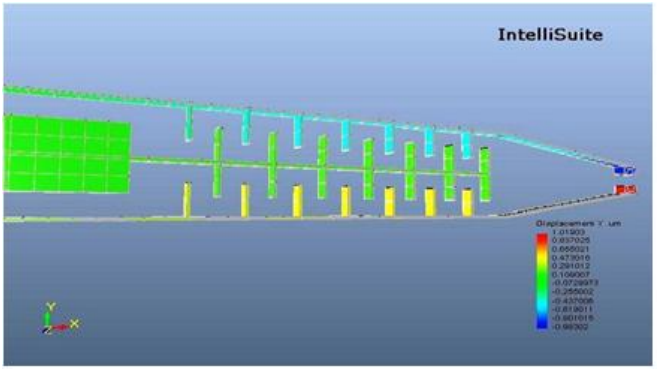

Figure 2: Simulation model of the microgripper with the rectangularfinger

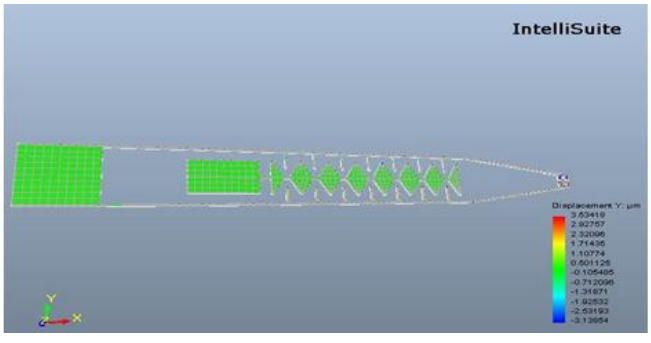

Figure 3: Simulation model of the microgripper with the tapered 1finger

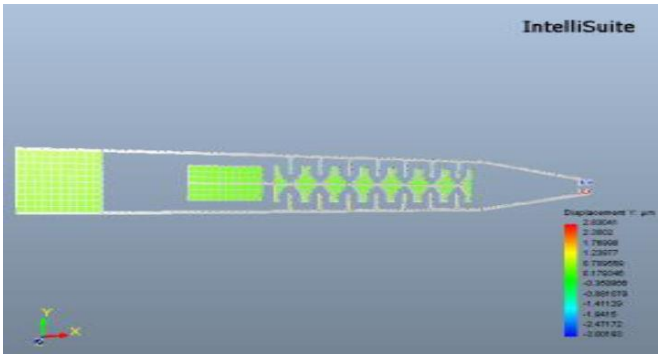

Figure 4: Simulation model of the microgripper with tapered 2 finger

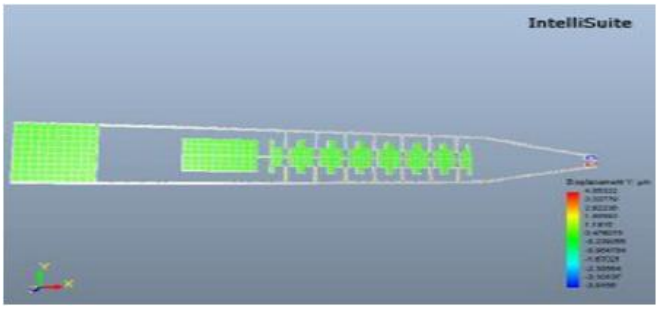

Figure 5: Simulation model of the microgripper with stepped finger

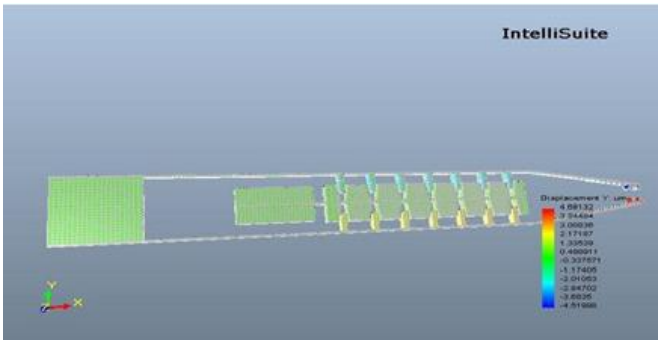

Figure 6: Simulation model of the microgripper with optimal finger

The simulation and analytical findings of the microgripper with various forms are compared in Table 2. The findings show that there is a fair degree of agreement between the two outcomes, with a maximum percentage error of 1.9 percent. By changing the finger forms, it was possible to increase displacement for a given voltage while maintaining a linear force profile, according to the findings. At a voltage of 14 volts, a displacement of around 1.9 m has been recorded for the rectangular finger. On the other hand, microgrippers with finger Tapered 1 and Tapered 2 forms have produced displacements of 3 m and 4.44 m at 14 volts. The microgripper with stepped finger form has a displacement of around 6.66 m. A displacement of 9 m is provided by the microgripper with the optimal

finger shape (Ye et al., 1998). As a consequence, among all the forms, the optimised finger shape-based design produces a superior displacement, as seen by the outcomes shown in Table 2.

Table 2: Comparison of the displacement of the microgrippers

Microgripper - Finger shape	Voltage (Volts)	Displacement (µm)		% Error
		FEM	Analytical	
Rectangular	14	1.92	1.885	1.8617
Tapered 1	14	3.04	2.99	1.6071
Tapered 2	14	4.44	4.3835	1.2888
Stepped	14	6.66	6.7318	1.0668
Optimal	14	9.09	8.9758	1.2728

Analysis of Microgripper with Load

The simulation results of a microgripper with load are shown in Table 3. Using the approach, 0.0312 Pa of load is supplied to the gripper to compute the force the microgripper will apply while carrying the weight.

Table 3: Comparison of the displacement of microgrippers with load

Microgripper (Finger shape)	Displacement (µm)		
	X	y	Z
Rectangular	0.027	0.8	0.00029
Tapered 1	0.003	2.98	0.1607
Tapered 2	0.2458	4.3	0.520
Stepped	0.2	6.52	0.161
Optimal	0.327	8.8	0.035

The in-plane displacement (y) is somewhat decreased with the application of load, as can be seen from a comparison of the microgripper's displacement results with and without load. The result also demonstrates that the load, which is applying force to the gripper, is significantly increasing the out of plane displacement (z). With this data, it is evident that the suggested gripper is performing well even under stress.

V-I Characteristics of Microgripper

On a N type SOI wafer, the microgrippers are created using the bulk micromachining process. In the same sample, microgrippers and cantilever beams are constructed.

Even though all of the devices were successfully constructed, their dimensions were such that, according to the analytical calculation, they produced a force on the order of piconewtons. Due to the characterisation facility's limitations, this could not be assessed.

No discernible movement could be seen when a voltage of up to 100 V was put across the microgripper because the grippers created a force on the order of pico-newtons. Thus, greater voltage excitation was needed in order to quantify such a little force and displacement. An analytical calculation revealed that in order to achieve a displacement of 2.6E-4 m, a voltage excitation of 2500 volts must be applied. In fact, a voltage sweep exceeding 100 volts was not supported by the device characterization facility. As a result, the intended microgripper's displacement could not be seen. Therefore, the current that generates force and displacement is monitored in order to evaluate the performance of the microgripper.

This research demonstrates that the optimised finger-shaped microgripper outperforms those built of other finger shapes because it generates more force for a given current. The optimum finger shape would produce a greater displacement since it creates more force among all the finger forms taken into consideration, even if the displacement cannot be physically detected.

Figure 7 displays the manufactured microgripper's SEM picture. Figure 8 provides a more detailed view of the manufactured microgripper. Voltage Vs. Current (V-I) characteristics for the device are acquired using the characterisation facility at CeNSE Laboratory, IISc.

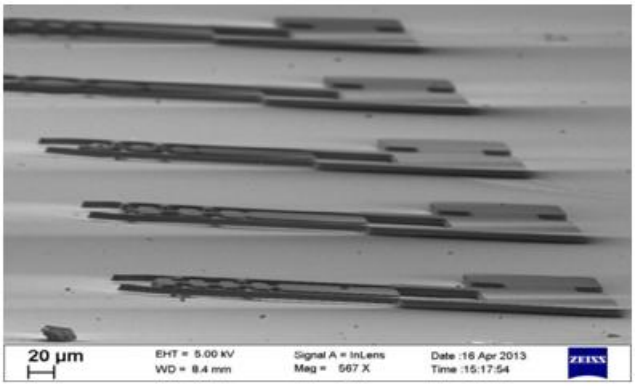

Figure 7: SEM Image of the fabricated microgripper with tapered 1finger (CeNSE Laboratory, IISc)

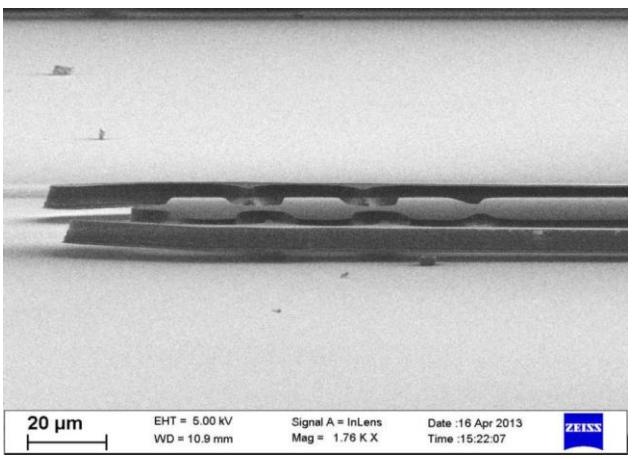

Figure 8 A closer look of the SEM Image of fabricated microgrippertapered 1 (CeNSE Laboratory, IISc)

The experimental setup of the 4-point probe station using which the V-I characteristics are obtained is shown in Figure 9. Figure 4.10 shows the simulation results of V-I characteristics of microgripper with different finger shapes. The comparison of the V-I characteristics obtained from the simulation and experimental results of the device of tapered 1 shaped microgripper is shown in Figure 11. The results fairly match each other.

From the figure 10, it could be seen that the current increases several hundreds of times from rectangular shape to tapered case and highest in the optimal case. This is due to the fact that the average current density (Current density = Current/Area) of the device is increasing manifold from rectangular to the optimal case as shown in Table 4

Table 4: Microgripper and its current density

Type of Microgripper	Average Current Density (A/m^2)
Rectangular	4.63403E-07
Tapered 1	1.97E-05
Tapered 2	5.93E-06
Stepped	8.78E-06
Optimal	1.18E-04

For the same applied voltage, the area of the cross-section of various kinds of fingers changes, which changes the current density as well. The area of the cross section stays constant for rectangular fingers. The current of a rectangular microgripper is thus smaller than that of other forms of microgripper since the change in current density is the same. Since the ideal finger has the smallest cross sectional area out of all of them, its average current density is also the greatest. Because of the average cross-sectional area's decline, the corresponding current density and therefore the current values increased. Figure 4.12's simulation findings, which illustrate this characteristic,

A simulation and experimental study are conducted on a parallel plate microgripper model. Using a four-point probe station, the parallel plate is subjected to a D.C. voltage sweep from 0 to 100 volts, and the accompanying current readings are recorded. As the supplied voltage is always D.C., the charging current first increased before becoming saturated once it achieved steady state. The V-I characteristics research assisted in analysing the trend of produced force with regard to the rise in current since force is proportional to the square of current and could not be measured due to its tiny size.

Figure 9: Four point probe station to obtain V-I characteristics(CeNSE Laboratory, IISc)

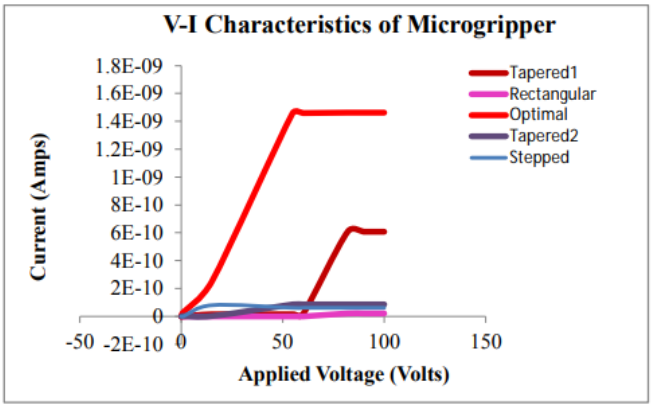

Figure 10: Simulated V-I characteristics of the various types ofmicrogrippers

Figure 11 compares the computational and experimental findings for the V-I characteristics of one kind of microgripper, a tapered 1 finger type. The findings' discrepancy may be caused by residual stress as well as by a number of manufacturing problems in the manufactured microgripper.

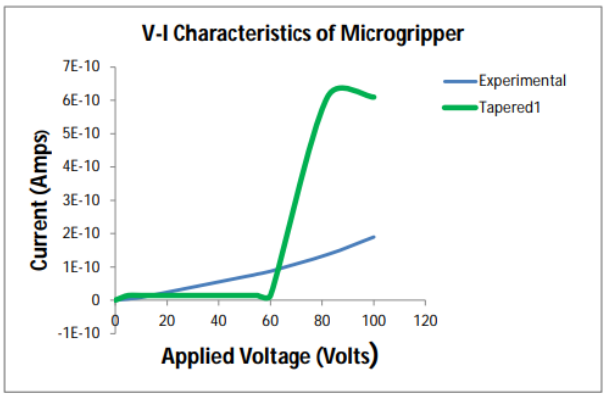

Figure 11: V-I characteristics of fabricated and simulated microgripper

Thus, after developing analytical models for each of the many finger shapes, the one that performs best is determined. For the creation of analytical models of various finger forms, a rectangular microactuator

with two jaws is being examined. The performance of the microactuator under load is also simulated, and the results are good. Now, the source of the rise in displacement is also validated by investigations on the V-I characteristics of several microgrippers. Using the proposed analytical model, the ideal finger-shaped microgripper providing the most displacement is also verified.

CONCLUSION

Earlier, the closed form models were used to do the pull-in analysis of the microgripper. The findings show once again that only one model accurately determines the pull-in voltage for a given range of size. When compared to electro thermal actuators, electrostatic actuation may provide excellent displacement, but it also needs high voltage to operate. In the realm of MEMS actuators, the usage of electro thermal actuators is highly regarded.

REFERENCES

1. Takahashi, H, Nagata, S, Odagiri, T & Kageyama, T 2018, 'Establishment of the cross-clade antigen detection system for H5 subtype influenza viruses using peptide monoclonal antibodies specific for influenza virus H5 hemagglutinin', Biochemical and biophysical research communications, vol. 498, no. 4, pp. 758-63.
2. Lang, HP, Hegner, M & Gerber, C 2017, 'Nanomechanical cantilever array sensors', in Springer Handbook of Nanotechnology, Springer, pp. 457-85.
3. Shoaib, M, Hamid, NH, Malik, AF, Ali, Z, Basheer, N & Tariq Jan, M 2016, 'A review on key issues and challenges in devices level MEMS testing', Journal of Sensors, vol. 2016.
4. Ruchika, AK 2015, 'Performance analysis of zinc oxide based alcohol sensors', Int. J. Appl. Sci. Eng. Res., vol. 4, no. 4, pp. 428-36.
5. Nallathambi, A & Shanmuganantham, T 2014, 'Performance analysis of cantilever based MEMS sensor for environmental applications', in 2014 International Conference on Smart Structures and Systems (ICSSS), pp. 118-22.
6. Sigmund O. (2011) Optimum Design of Microelectromechanical Systems. In: Aref H., Phillips J.W. (eds) Mechanics for a New Mellennium. Springer, Dordrecht. https://doi.org/10.1007/0-306-46956-1_33
7. Joglekar MM & Pawaskar DN. Closed - form empirical relations to predict the dynamic pull-in parameters of electrostatically actuated tapered microcantilevers. Journal of micromechanical microengineering, 2011; vol. 21: pp. 1-12.
8. Ananthasuresh GK. Electro Thermal-compliant Microactuator Hands on SOI MUMPs Workshop, June 17-18, 2011.
9. COMSOL 4.2 a. Joule heating module, http://www.comsol.com, 2011.
10. Haluzan DT, Klymyshyn DM, Achenbach S, Börner M. Reducing Pull-in voltage by adjusting gap shape in electrostatically actuated cantilever and fixed- fixed beams, Micromechanics, 2010; Vol. 1: pp. 68-81.
11. Khan K, Shafaat AB &Sohail M. Design, implementation and testing of electrostatic SOI MUMPs based microgripper. Microsystems Technology, 2 0 1 0 ; vol. 16: pp. 1957-1965. DOI 10.1007 / s 00542-010-1129-2.

Corresponding Author

Shubham Dubey*

Research Scholar, Shri Krishna University, Chhatarpur M.P.